Wide-field spatio-spectral interferometry for far-infrared space applications

David Leisawitz,[a] J. Thomas Armstrong,[b] Matthew R. Bolcar,[a] Richard G. Lyon,[a] Stephen F. Maher,[a,c] Nargess Memarsadeghi,[a] Stephen A. Rinehart,[a] and Evan J. Sinukoff[d]

[a] NASA Goddard Space Flight Center; [b] Naval Research Laboratory; [c] SSAI, Inc.; [d] Institute for Astronomy, University of Hawaii and former co-op student at NASA GSFC

The NASA Astrophysics Roadmap includes a space-based far-IR interferometer in the 2020s, as well as several later interferometry missions for which a far-IR interferometer sets the stage. Such a mission has been steadfastly recommended by the far-IR community for over a decade, as multiple high-priority science goals demand high sensitivity, spectroscopy, and imaging in the spectral range ~ 25 - 400 μm with sub-arcsecond angular resolution (see SPIRIT poster), better than that practically attainable by any other means.

The three major enabling technologies for a far-IR interferometry mission are: low-noise, high-speed detectors in small (~16^2 pixel) arrays; a demonstrated capability to cool optical system components to ~4 K and focal planes to tens of mK with cryo-coolers; and the spatio-spectral interferometry ("double Fourier") technique through which wide-field integral field spectroscopic data can be derived from interferometric measurements.

This poster reports on the current status of wide-field spatio-spectral interferometry and plans for maturation of the technique to space-flight readiness. Thus far, relatively simple spatial-spectral test patterns have been observed with the Wide-Field Imaging Interferometry Testbed (WIIT) at NASA's Goddard Space Flight Center, and hyperspectral image cubes representing the observed scenes have been constructed based on the measured interferograms. A critical future milestone is the accurate construction of an astronomically realistic, spatially and spectrally complex scene.

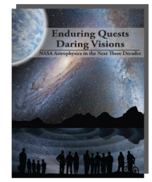

NASA Astrophysics Roadmap

"FIR interferometry [is] a logical starting point that provides a useful training ground while delivering crucial science."

Far-IR Community Plan (2009)

"Our long-term goal for the 2020-2035 era is a program of sensitive imaging and spectroscopic observations capable of resolving small-scale cosmic structure across the entire FIR/SMM range. This will require ... a cooled FIR/SMM spatial interferometer...."

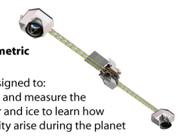

The Space Infrared Interferometric Telescope (SPIRIT)

A Probe-class far-IR mission designed to:

- ❐ image protoplanetary disks and measure the distributions of water vapor and ice to learn how the conditions for habitability arise during the planet formation process;
- ❐ image structures in a large number of debris disks to find and characterize unseen exoplanets; and
- ❐ make profound contributions to our understanding of the formation, merger history, and star formation history of galaxies.

What is wide-field spatio-spectral interferometry?

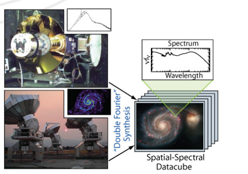

Spatio-spectral interferometry combines the capabilities of an imaging interferometer (bottom left) with those of a Fourier Transform Spectrometer (top left) to produce hyperspectral image cubes. A detector array measures multiple "primary beams" simultaneously, widening the field of view relative to that of a conventional Michelson interferometer.

The Wide-field Imaging Interferometry Testbed (WIIT) works at visible wavelengths for convenience and to save cost, but it is functionally and operationally equivalent to the space-based far-IR interferometer SPIRIT.

The performance parameters of the WIIT are well-matched to science-driven far-IR interferometer mission requirements.

Parameter	SPIRIT Requirements	WIIT Performance: Typical Experiment	WIIT Performance: Full Capability
Field-of-View	1 arcmin (14 pixels)	1.2 arcmin (30 pixels)	2.5 arcmin (64 pixels)
Angular Resolution	0.3 arcseconds	0.3 arcseconds	0.3 arcseconds
Spectral Resolution	$R \equiv \lambda/\Delta\lambda = 3000$	R ~ 200	R > 3000
Instrumental Visibility	V = 0.94 (A & WFE)*	V = 0.84 (A & WFE)*	V = 0.84 (A & WFE)*
Sensitivity	Photon-noise limited	Photon-noise limited	Photon-noise limited

* Dominant visibility loss terms are alignment (A) and wavefront error (WFE)

Calibrated Hyperspectral Image Projector (CHIP)

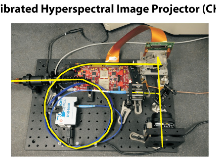

The CHIP uses Digital Light Processing (DLP) technology to produce the customized, spectrally-diverse scenes we observe in the lab. CHIP scenes have spatial resolution finer than that resolvable with the interferometer. Each CHIP pixel can take on a unique spectrum in the wavelength band 0.38 - 1.6 μm, with approximately 5-nm spectral resolution. Spectral calibration is achieved with an onboard fiber-coupled spectrometer. The yellow line in the photograph above traces the optical path through the system. See Bolcar *et al.* 2012 for details.

Schematic view of the WIIT

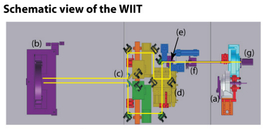

(a) Light source *
(b) Parabolic mirror
(c) Baseline mirrors (2)
(d) Optical delay stage
(e) Beamsplitter (combiner)
(f) Lens system
(g) Camera

* Calibrated Hyperspectral Image Projector (CHIP)

Objectives and Methodology

The goal of this project is to develop the wide-field spatio-spectral interferometry technique to NASA Technology Readiness Level (TRL) 6 from its current readiness level 5 for the space-based far-IR interferometer SPIRIT (see panel to the right). This is somewhat analogous to the maturation of Wavefront Sensing and Control for JWST. Specifically, our aim is to demonstrate wide-field spatio-spectral interferometry in a relevant environment with a laboratory testbed, characterize all error and noise terms relevant to space-based far-IR interferometry, and produce spatio-spectral synthesis software capable of processing data from a mission like SPIRIT.

The figure below illustrates key elements of our approach (Leisawitz *et al.* 2012), which can be summarized as follows:

- ❐ Observe astronomically realistic test scenes with an optical scale model (hardware testbed) equivalent to SPIRIT in terms of functionality, operation, and factors that limit data quality.
- ❐ Compare observed interferograms with those predicted by a high-fidelity computer model of the testbed in which error terms associated with individual hardware components are modeled and can be switched on or off. Understand and document the effects of all significant error terms and sources of fringe visibility loss.
- ❐ Compare hyperspectral image cubes derived from the interferometric data with "truth images" of the observed test scenes. Explain residual differences between the derived output and the measured input images in terms of factors relevant to a far-IR interferometer in space, such as imperfect optical system alignment, optical components and detectors, undersampling of the spatial Fourier components, photon noise, motion smearing due to interferometer rotation, and artifacts associated with image construction.

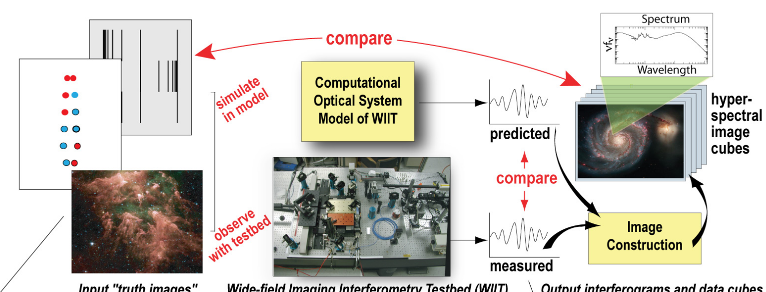

The testbed's performance is well understood

Sources of Visibility Loss in WIIT

Source	Parameter ID	Parameter Value	Visibility Formula	Visibility Value
Alignment				
Coalignment at pupil	$1-\eta$	0.975	$1-\eta$	0.975
Tip/tilt at exit pupil	α	0.5"	$2J_1(\pi D\alpha/\lambda)/(\pi D\alpha/\lambda)$	0.995
Optics (RMS wavefront error)				
Collimating mirror	δ	15.75 nm	$\exp[-2\pi\delta/\lambda]^2$	0.97
Beamsplitter	δ	15 nm	$\exp[-2\pi\delta/\lambda]^2$	0.98
Interferometer mirrors	δ, N	10 nm, 9 mirrors	$\exp[-2N\pi\delta/\lambda]^2$	0.92
Intensity Mismatch	ρ	92%	$2/(\rho^{1/2}+\rho^{-1/2})$	0.999
Positional Knowledge	δx	9.89 nm	$\mathrm{sinc}(2\pi\delta x/\lambda)$	0.999
Frame Exposure Time	t_{obs}	100 ms	$\mathrm{sinc}(2\pi v_{stage} t_{obs}/\lambda)$	0.9995
Total Visibility Loss				0.84

Imperfect mirrors are the dominant source of fringe visibility loss. The visibility measured in the lab on an unresolved point source is 0.84, as predicted (table above).

Sources of Visibility Uncertainty in WIIT

Source	Parameter ID	Parameter Value	Visibility Uncertainty Formula	Visibility Uncertainty Value
Light Source	$\delta I/I$	<0.5%	$\delta I/I$	<0.71%
Camera				
Bit Noise	σ_{bit}	0.5 counts	σ_{bit}/N_{cnts}	0.011%
Photon Counting	N_{elec}	2×10^{5} e^-	$[(2/N_{elec})(2^{16}/N_{cnts})]^{1/2}$	1.40%
Camera noise (read noise, dark current)	σ_{det}	15 e^-	$(2\sigma_{det}/N_{elec})(2^{16}/N_{cnts})$	0.22%
Total Visibility Uncertainty				1.59%

The visibility uncertainty, typically ~2%, is dominated by photon noise.

Representative testbed data

A combination of spatial and spectral information is encoded in the interferograms

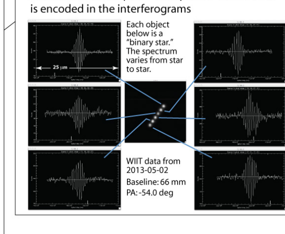

Comparison of measured and predicted interferograms

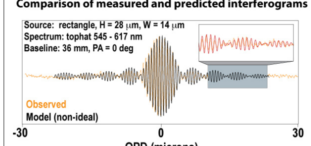

Our computational optical system model SsICOM predicts interferograms that closely match those seen in the lab. In the model, error sources can be activated individually, all at once ("non-ideal," as above), or deactivated to predict the performance of an ideal interferometer.

Hyperspectral image construction

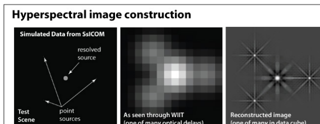

(Above) Spatio-Spectral Synthesis Software (S4) processing of synthetic data from the computational optical system model SsICOM. Only 0, 45, 90, and 135 deg baseline measurements were simulated, accounting for the star-shaped "dirty beam." CLEAN deconvolution can be used to remove these artifacts, but they only appear when the *u-v* plane is sparsely sampled. The reconstructed image (right) is one of many drawn from the output cube representing the test scene.

(Right) Real data from WIIT and corresponding S4 processing results. In this case the *u-v* plane was densely sampled and the reconstructed image is virtually free of artifacts.

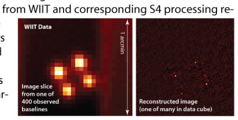

Future Plans

During the next two years, we aim to:

- ❐ demonstrate excellent agreement between synthesized hyperspectral data cubes and observed, astronomically realistic "truth images";
- ❐ quantitatively account for any measured differences in terms of understood instrumental effects; and
- ❐ complete and verify the performance of a hyperspectral image construction algorithm.

Bolcar, M.R., Leisawitz, D., Maher, S., and Rinehart, S., "Demonstration of the Wide-field Imaging Interferometer Testbed using a Calibrated Hyperspectral Image Projector," in Optical and Infrared Interferometry III. Proceedings of the SPIE, Volume 8445, article id. 84452D (2012)

Leisawitz, D. et al., "Developing wide-field spatio-spectral interferometry for far-infrared space applications," in Optical and Infrared Interferometry III. Proceedings of the SPIE, Volume 8445, article id. 84450A (2012)